

Communications





How to cite: *Angew. Chem. Int. Ed.* **2023,** *62*, e202303115 International Edition: doi.org/10.1002/anie.202303115 German Edition: doi.org/10.1002/ange.202303115

Upcycling of Polybutadiene Facilitated by Selenium-Mediated Allylic Amination

Mercie N. Hodges, Matthew J. Elardo, Jinyoung Seo, Alexander F. Dohoda, Forrest E. Michael, and Matthew R. Golder*

Abstract: Accumulation of end-of-life plastics presents ongoing environmental concerns. One strategy to solve this grand challenge is to invent new techniques that modify post-consumer waste and impart new functionality. While promising approaches for the chemical upcycling of commodity polyolefins and polyaromatics exist, analogous approaches to repurpose unsaturated polymers (e.g., polybutadiene) are scarce. In this work, we propose a method to upcycle polybutadiene, one of the most widely used commercial rubbers, via a mild, metal-free allylic amination reaction. The resulting materials have tunable thermal and surface wetting properties as a function of both sulfonamide identity and grafting density. Importantly, this approach maintains the parent alkene microstructure without evidence of olefin reduction, olefin transposition, and/or chain scission. Based on these findings, we anticipate future applications in the remediation of complex elastomers and vulcanized rubbers.

In the United States, 75% of all plastic consumed ends its life in a landfill. An additional 16% is combusted for energy, while only 9% is repurposed through downcycling, closed-loop recycling, or upcycling. [1-6] Polymer upcycling, or chemical modification to create value-added materials, is a promising way to mitigate plastic waste. Post-polymerization modification (PPM) of existing post-consumer plastic is a common approach to upcycle commodity materials [7-11] without needing to design novel monomers for depolymerization-repolymerization strategies. [12-15]

Recently, strategies for the functionalization of polystyrene, [16] polyolefins, [17-20] polyethers, [21] polylactides, [22] and polyacrylates [23,24] have evolved concurrently with the modernization of synthetic organic methodology. [25] Advances in C H activation, [8] (photo) redox catalysis, [21,26,27] and organocatalysis [17,18] have enabled the streamlined synthesis of previously inaccessible macromolecules from post-con-

[*] M. N. Hodges, M. J. Elardo, A. F. Dohoda, Prof. Dr. F. E. Michael, Prof. Dr. M. R. Golder Department of Chemistry, University of Washington 36 Bagley Hall, Seattle, WA 98195 (USA) E-mail: goldermr@uw.edu

I Seo

Department of Chemistry & Chemical Biology, Harvard University 12 Oxford Street, Cambridge, MA 02138 (USA)

Angew. Chem. Int. Ed. 2023, 62, e202303115 (1 of 6)

sumer plastics. On the other hand, fewer examples exist for the direct upcycling of unsaturated rubbers (e.g., polybutadiene, polyisoprene), the main constituents in consumer tires. Approximately 1 billion tires are discarded each year, but major processing strategies still rely on landfilling, pyrolysis, and downcycling (e.g., asphalt filler). [28–30]

Direct polydiene upcycling is especially challenging due to the high reactivity of the carbon-carbon π -bond relative to alternative functionalization pathways. For example, polybutadienes are readily converted to saturated materials via alkene difunctionalizations^[31–36] that imbue the resulting polyolefin products with diverse functional groups at the expense of saturation (Figure 1A). An alternative approach to modify polydienes utilizes olefin transposition reactions to retain backbone unsaturation. For example, treatment with triazolinediones of hypervalent iodine

(A) Previous Work: 1,4-Polybutadiene Functionalizations

(B) Precedence: Small Molecule Allylic Amination

(C) This Work: Direct Polybutadiene Upcycling

Figure 1. A) Evolution of 1,4-polybutadiene functionalization and B) allylic C H amination conditions that inspired (C) this polybutadiene upcycling work.

3213773, 2023, 20, Downloaded from https://onlinelibrary.wiley.com/doi/10.1002/anie 20233115 by University Of Washington, Wiley Online Library on [2207/2023]. See the Terms and Conditions (https://onlinelibrary.wiley.com/rems-and-conditions) on Wiley Online Library for rules of use; OA articles are governed by the applicable Creative Commons License

compounds^[41] affords functionalized polydienes, albeit with concomitant alkene migration. Because microstructure in unsaturated polymers can influence physical properties, [42-44] it would be advantageous to retain the original 1.4-diene microstructure following upcycling.

To overcome this long-standing challenge, in this work we demonstrate the first example of direct 1,4-polybutadiene upcycling through a metal-free C H allylic functionalization reaction inspired by recent work on terpenoid functionalization (Figure 1B).[45] Importantly, this seleniumcatalyzed amination process maintains the parent 1,4-diene backbone without detectable chain scission, crosslinking, and/or alkene transposition. Sulfonamide functionality is introduced directly to the native backbone without preincorporation of designer monomers; the functionalized polymers reported herein would be difficult to synthesize via alternative synthetic routes. Through methodology development for 1,4-polybutadiene upcycling via grafting sulfonamides (PUGS) we find that both sulfonamide identity and density (Figure 1C) can modulate thermal and surface wetting properties as assessed by differential scanning calorimetry and drop shape analysis.

To begin, we synthesized low molar mass (M_{n,MALS} = 15-20 kDa) telechelic-functionalized 1,4-polybutadiene (1,4-PBD) (ca. 77 % trans, Figures S38 and S39) via ring-opening metathesis polymerization (ROMP) of 1,5-cyclooctadiene (COD) and a cis-alkene chain transfer agent (Table S1).[46,47] ROMP enables strict formation of PBD devoid of 1,2-vinyl branched isomers and establishes well-defined chain ends; both structural features allowed for simplified structural analysis following PPM using NMR spectroscopy. Initial conditions for 1,4-PBD amination were based on recent successful examples of allylic terpenoid functionalization. [45] Specifically, 1,4-PBD and sulfonamide were subjected to catalytic selenium (i.e., selenourea or phosphine selenide) and PhI(OAc)₂ (Figure 2A). We envisioned that perturbations to sulfonamide identity could impact bulk properties of PUGS materials. Initial efforts focusing on tosyl sulfonamide (TsS) and nosyl sulfonamide (NsS) functionalization of silyl ether-capped 1,4-PBD revealed broadened diagnostic aromatic (7.6-7.8 ppm) signals by ¹H NMR spectroscopy (Figures S21-S25). We confirmed that these results were not due to sulfonamide intercalation with 1,4-PBD by rigorously purifying all samples with preparative-scale gel permeation chromatography (GPC) (Figure S1). Sulfonamide densities ranging between $D_{NMR} = 9.0-64 \text{ mol } \% \text{ [Eqs. (S4) and (S5)]},$ as assessed by ¹H NMR spectroscopy analysis (Figure 2B), were obtained by varying the catalyst and/or sulfonamide identity (Table 1). With promising initial amination results on a lower molar mass polymer sample, we turned our attention to higher molar mass 1,4-PBD (M_{n,MALS} = 32 kDa) (Table S1) for more challenging upcycling using trifluoromethane sulfonamide (TFMS) and trifluoropropyl sulfonamide (TFPS). Polymer semifluorination is known to engender the resulting materials with novel thermal and surface coating properties.^[48] Subsequent ¹⁹F NMR spectroscopy analysis (Figure 2C) of upcycled telechelic 1,4-PBD bearing trifluoromethyl phenyl chain ends (Figure S33-S36) revealed sulfonamide densities ranging between $D_{NMR} = 5.4-41 \text{ mol}\%$

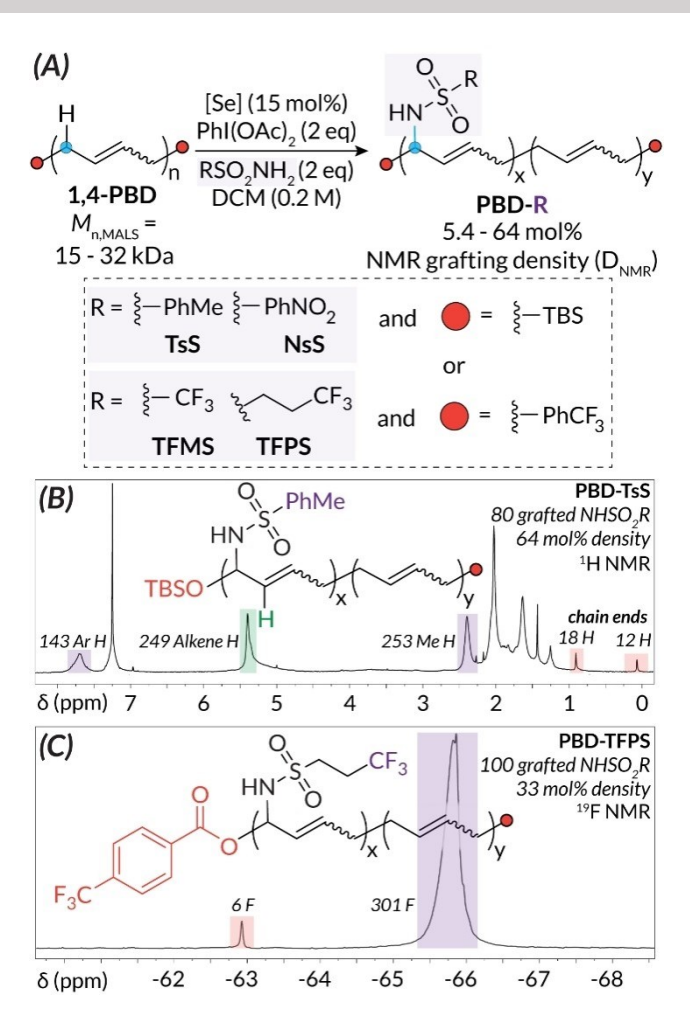


Figure 2. A) Scope of 1,4-PBD upcycling ([Se] = IMeSe or PCy₃Se). [Se], PhI(OAc)₂ and RSO₂NH₂ relative to PBD monomer units. B) Sample ¹H NMR spectrum used to assess grafting density of PBD-TsS. C) Sample 19F NMR spectrum used to assess grafting density of PBD-TFPS

[Eqs. (S1)-(S3)]. We attempted to corroborate these NMR spectroscopy data with complementary absolute molar mass determination using analytical GPC coupled with a multiangle light scattering (MALS) detector, but these data proved to be unreliable. We surmise that this issue is due to self-assembly or aggregation of the upcycled polymers (i.e., via hydrogen bonding) and/or analyte interaction with the GPC columns; counterintuitive increases in retention time (Figures S6–S13) relative to 1,4-PBD samples of comparable length (Figures S3-S4) despite an increase in PUGS molar mass support these hypotheses (Table S2).

Upcycled materials with higher densities (>20 mol%) generally were isolated with shorter average chain lengths, as assessed by ¹H NMR spectroscopy, relative to parent 1,4-PBD chain lengths. We surmise that chain aggregation (see above) complicated purification during preparative GPC and ultimately resulted in artificial molar mass fractionation. Nonetheless, the average chain lengths of lower density upcycled polymers were generally in good agreement with parent 1,4-PBD chain lengths, demonstrating that this allylic





Table 1: Analytical characterization data of upcycled 1,4-polybutadienes.

Sulfonamide	[Se]	$D_{NMR} [mol \%]^{[a]}$	$D_{TGA}[mol\%]^{^{[b]}}$	$T_{g} [^{\circ}C]^{[c]}$	$\Theta \ [^{\circ}]^{[e]}$
None	N/A	0	0	24 ^[d]	82–84 ^[f]
NsS	IMeSe	9.0	10	18 49 ^(d) 21 15 21 4.3 15 ^(d) 25	86
NsS	PCy₃Se	22	15		88
TsS	IMeSe	29	18		87
TsS	PCy₃Se	64	46		79
TFMS	PCy₃Se	14	15		83
TFMS	IMeSe	41	34		90
TFPS	IMeSe	5.4	5.9		94
TFPS	PCy₃Se	33	31		85

Synthesized using [Se] (15 mol%), PhI(OAc)₂ (2 equiv) and RSO₂NH₂ (2 equiv), all relative to PBD monomer units, in CH₂Cl₂ (0.2 M). [a] NMR grafting density determined by ¹H NMR spectroscopy or ¹⁹F NMR spectroscopy. [b] Thermogravimetric analysis (TGA) grafting density. [c] Determined by differential scanning calorimetry (DSC), 2nd heating at 5 °C/min. [d] No T_g observed, only T_m observed. [e] Determined by drop shape analysis (average of three measurements). [f] For 1,4-PBD with PhCF₃ chain ends θ = 82°, for 1,4-PBD with TBS chain ends θ = 84°.

functionalization reaction does not result in chain cleavage (Table S2). Furthermore, across all PUGS samples, alkene stereochemistry does not change significantly following amination (68-85% trans, Figures S41-S44) compared to the parent 1,4-PBD samples (ca. 77% trans, Figures S38-S39). To demonstrate compatibility with industrially-relevant elastomers, we also performed PUGS using TsS (15 mol% SePCy₃) on commercial PBD (PBD-SA, $M_{n,MALS} = 5.7 \text{ kDa}$, $T_g = 96 ^{\circ}\text{C}$) containing 13 % 1,2-vinyl linkages (Figure S40) solid PBD-SA-TsS was obtained following purification. Overall, these collective PUGS materials serve as representative examples from which to probe the impact of sulfonamide identity and density of backbone incorporation on subsequent physical properties by thermogravimetric analysis (TGA), differential scanning calorimetry (DSC), and drop shape analysis (Table 1).

We next assessed the thermal stability of **PUGS** samples via TGA (Figures S48-S56). While the appended sulfonamide functionality led to a decrease in the onset of decomposition temperature $(T_{d,10\%})$, we were able to correlate structural features with thermal decomposition profiles. Parent 1,4-PBD shows a single $T_{d,10\%}$ = 386 °C whereas upcycled PBD samples generally show two separate decomposition events. Depending on the sulfonamide density and identity, the first onset between $T_{d,10\%}$ = 194 °C to $T_{\rm d,10\%}$ = 310 °C corresponds to the temperature where sulfonamide functionality begins decomposing from the backbone (Figure 3A). A second decomposition onset is observed near 386°C as the PBD backbone begins decomposing. The mass loss between these two events represents the approximate mass attributed to grafted sulfonamide functionality. Conversion from mass loss to sulfonamide density (mol%) [Eqs. (S6)-(S11)] leads to functionalization values (D_{TGA}) that are in good agreement with sulfonamide densities calculated by NMR spectroscopy (D_{NMR}) (Table 1 and Tables S2).

Prior to decomposition, 1,4-PBD has rich thermal properties depending on the olefin microstructure. Predominantly *cis*-1,4-PBD is crystalline with a melt below room temperature ($T_{\rm m}$ = ca. 1 °C). As *cis* content decreases, the corresponding melt temperature increases to above 100 °C. As is typical for *trans*-rich 1,4-PBD devoid of 1,2-

vinyl branching, our parent 1,4-PBD samples (ca. 77 % trans, Figures S38 and S39) have an observable melt at $T_{\rm m}$ = 24°C^[52] with no observable glass transition as assessed by DSC measurements to 173°C (Figure S66). Analysis of upcycled 1,4-PBD samples by DSC (Figures S58-S65) reveals thermal transitions that depend on sulfonamide density and identity. At the lowest sulfonamide density, PBD-TFPS (5.4 mol%) retains a melt near room temperature (T_m=15°C); thermal properties are not drastically influenced. At higher sulfonamide densities, however, such as PBD-NsS (9.0 mol%), the upcycled material is amorphous with $T_g = 18$ °C. When higher densities of NsS were used to access PBD-NsS (22 mol%), only a single melt was observed ($T_{\rm m}$ = 49 °C). These data are in stark contrast to those of structurally similar PBD-TsS (29 mol%) which is amorphous with $T_g = 21 \,^{\circ}\text{C}$.

We hypothesize that at higher NsS densities, hydrogen bonding via the nitrophenyl acceptor results in sidechain crystallization. Hence, by simply modulating the hydrophobicity and/or polarizability of the sulfonamide, vastly different thermal properties can be achieved relative to unfunctionalized 1,4-PBD. When the identity of the sulfonamide remains constant, we observe a general increase in transition temperature as sulfonamide density increases. For example, for PBD-TsS, $T_g = 21$ °C at 29 mol % and increases to $T_g = 15$ °C at 64 mol% (Figure 3B). Similarly, for **PBD-TFMS**, $T_g = 21$ °C at 14 mol% and increases to $T_g =$ 4.3 °C at 41 mol%, while for **PBD-TFPS** $T_{\rm m}$ = 15 °C at 5.4 mol% and increases to $T_g = 25$ °C at 33 mol% (Fig-ure 3C). Our work demonstrates that PBD thermal properties can be tuned using PUGS, even at low sulfonamide densities, without altering microstructure.

On the other hand, by incorporating even low degrees of 1,2-vinyl branching (<10%), PBD becomes amorphous with a T_g = 96°C (e.g., **PBD-SA**, 13% vinyl). The impact of 1,2-branching, the amount of which remains unchanged after **PUGS** (Figure S25), becomes apparent with an increase in T_g for **PBD-SA-TsS** (69 mol%) ($T_g \Box 50$ °C) relative to similar 1,4-PBD analog **PBD-TsS** (64 mol%) ($T_g = 15$ °C). A small molecule competition experiment (Scheme S1 and Figure S80) demonstrates that secondary allylic C H positions (i.e., adjacent to the internal olefin of a 1,4-PBD



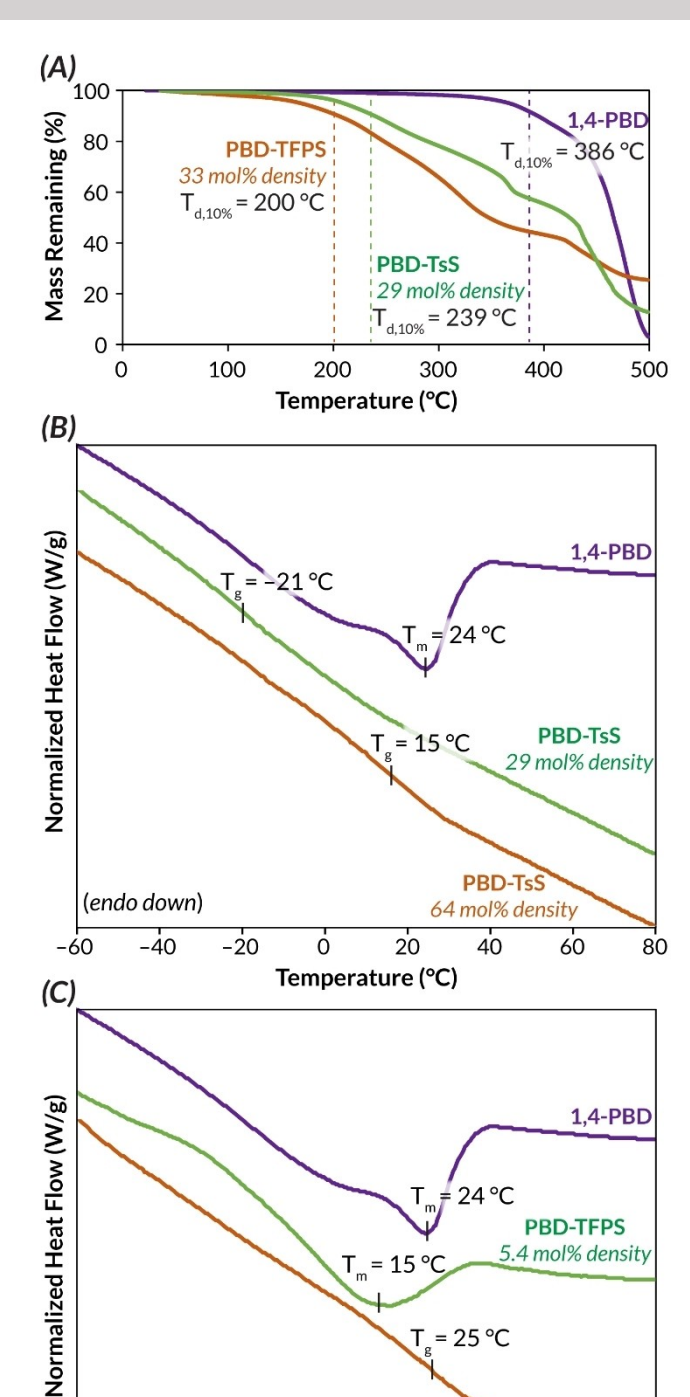


Figure 3. A) TGA curves of PBD-TsS and PBD-TFPS compared to 1,4-PBD. B) DSC curves of PBD-TsS samples compared to 1,4-PBD. C) DSC curves of PBD-TFPS compared to 1,4-PBD. All grafting densities refer to $D_{\rm NMR}$.

ó

20

Temperature (°C)

PBD-TFPS

33 mol% density

40

60

80

backbone) are more reactive than tertiary allylic C H positions (i.e., adjacent to the terminal olefin of a 1,2 vinyl branch). These data suggest that although it is feasible for

PBD-SA-TsS (69 mol%) to have *some* sulfonamide incorporation at tertiary sites, quantification is below the detection limits of NMR spectroscopy.

Polymeric coatings find broad utility in surface modulation by modifying substrate functionality, wettability, adhesion, and reactivity. [53-55] To explore the implications of 1,4-PBD upcycling on coating applications, we hypothesized that post-polymerization modification could impact wettability. We assessed how PUGS influences surface properties of hydrophobic 1,4-PBD by measuring water contact angles (θ) of spin-coated silicon wafers using a drop shape analyzer (Figures S68-S77). The sulfonamides chosen for our studies are amphiphiles; the sulfonamide moiety is inherently hydrophilic but is capped by a hydrophobic hydrocarbon or semifluorinated group. Drop shape analysis and subsequent one-way ANOVA test reveals density-dependent materials properties based on the bipolar nature of the sulfonamides (Figures S78-S79). At lower sulfonamide densities, we generally observe higher θ relative to that of 1,4-PBD (θ = 82-84°) (Figure 4A); these data indicate an increase in hydrophobicity as sulfonamide grafting seemingly increases surface roughness and hence θ . [56] As sulfonamide density increases further, we generally observe a counterintuitive decrease in θ (i.e., increasingly hydrophilic surface). For example, PBD-TFPS (5.4 mol%) is significantly more hydrophobic (p < 0.001) ($\theta = 94^{\circ}$) (Figure 4B) than 1,4-PBD but PBD-TFPS (33 mol%) shows no statistically significant difference in θ (θ =85°) compared to that of 1,4-PBD (θ = 82°). A similar trend is observed when non-fluorinated TsS or NsS are used; PBD-TsS (29 mol%) reveals no statistically significant difference (θ =87°) in θ relative to that of 1,4-PBD (Figure 4C) but PBD-TsS (64 mol%) is significantly more hydrophilic (p < 0.001) ($\theta = 79^{\circ}$) (Figure 4D) than 1,4-PBD (θ =84°). As sulfonamide density increases, however, hydrogen bonding between neighboring sulfonamides[49]

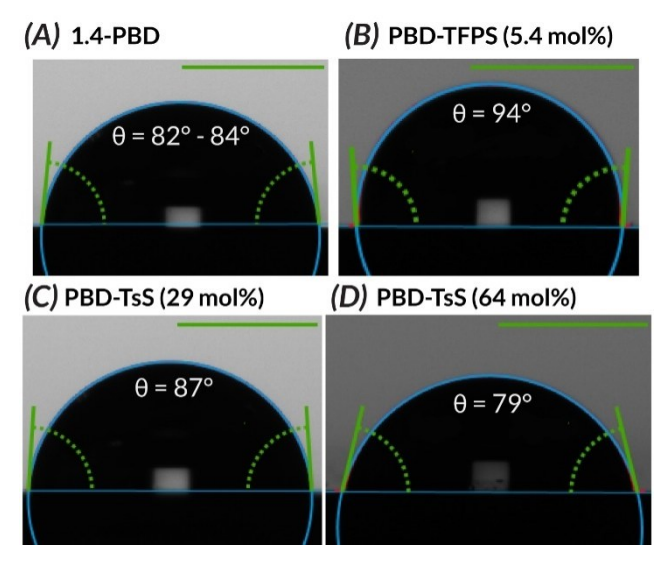


Figure 4. Water contact angles (θ) of A) 1,4-PBD and B)–D) upcycled 1,4-PBD ($D_{\rm NMR}$ listed) as measured by drop shape analysis. Reported water contact angles are an average of measurements on three separate water droplets on an SiO₂ surface. Scale bars = 2 mm.

(endo down)

-60

-40

-20

3213773, 2023, 20, Downloaded from https://onlinelibrary.wiley.com/doi/10.1002/anie 20233115 by University Of Washington, Wiley Online Library on [2207/2023]. See the Terms and Conditions (https://onlinelibrary.wiley.com/rems-and-conditions) on Wiley Online Library for rules of use; OA articles are governed by the applicable Creative Commons License



and/or water may result in burying of the hydrophobic tails to ultimately increase surface hydrophilicity.

PBD-TFMS samples are distinct outliers to the trend as hydrophobicity *increases* as a function of **TFMS** density. At lower sulfonamide density, **PBD-TFMS** (14 mol%) shows no statistical difference in θ (θ =83°) relative to that of 1,4-PBD (θ =82°), but unlike other examples (see above), at higher densities **PBD-TFMS** (41 mol%) is significantly more hydrophobic (p<0.001) (θ =90°) than 1,4-PBD. We surmise that the more acidic nature of **TFMS** (pK_a =ca. 7) may result in differences to film assembly and/or surface roughness in **PBD-TFMS** relative to other **PUGS** samples (pK_a =ca. 15). Overall, the ability to modulate wettability as a function of both sulfonamide density and identity (Figures S78 and S79) presents opportunities for the development of novel flexible coatings and soft materials with tunable surface hydrophilicities.

In summary, we demonstrate the utility of PUGS, a mild, selenium-catalyzed allylic amination process that engenders previously unrealized materials from prevalent polybutadiene elastomers with and without 1.2-vinyl branching. Importantly, the underlying mechanism that drives PUGS necessitates retention of the parent diene backbone without olefin saturation and/or transposition. Control over grafting density, as assessed by NMR spectroscopy and thermogravimetric analysis, of diverse sulfonamides provides a versatile platform from which to modulate thermal transitions. Furthermore, the amphiphilic nature of sulfonamides provides an opportunity to increase or decrease surface wettability as a function of grafting density. Combined, these results reveal how judicious selection of sulfonamide identity and density for PUGS permits decoupled thermal and surface properties in the final materials. Our collective work not only provides a viable solution for the direct upcycling of polybutadienes, but also for the future development of post-polymerization modifications on more complex elastomers (e.g., styrene-butadiene-styrene) and surface modifications of vulcanized rubbers.

Acknowledgements

This work was supported by generous start-up funds from the University of Washington. Dr. Wei-Pin Teh is thanked for experimental assistance. M.N.H. acknowledges the University of Washington Clean Energy Institute for a graduate research fellowship. Prof. Dianne Xiao is acknowledged for use of a thermogravimetric analyzer. Differential scanning calorimetry instrumentation is funded by the Student Technology Fund (STF) at the University of Washington. This material is based in part upon work supported by the state of Washington through the University of Washington Clean Energy Institute.

Conflict of Interest

The authors declare no conflict of interest.

Data Availability Statement

The data that support the findings of this study are available in the Supporting Information of this article.

Keywords: C H Functionalization · Polymers · Post-Polymerization Modification · Selenium · Upcycling

- [1] A. R. Rahimi, J. M. Garciá, Nat. Chem. Rev. 2017, 1, 0046.
- [2] N. Singh, D. Hui, R. Singh, I. P. S. Ahuja, L. Feo, F. Fraternali, Composites Part B 2017, 115, 409–422.
- [3] S. C. Kosloski-Oh, Z. A. Wood, Y. Manjarrez, J. P. De Los Rios, M. E. Fieser, *Mater. Horiz.* 2021, 8, 1084–1129.
- [4] B. A. Helms, T. P. Russell, Chem 2016, 1, 816-818.
- [5] T. H. Epps, L. T. J. Korley, T. Yan, K. L. Beers, T. M. Burt, JACS Au 2022, 2, 3–11.
- [6] Z. R. Hinton, M. R. Talley, P. A. Kots, A. V. Le, T. Zhang, M. E. MacKay, A. M. Kunjapur, P. Bai, D. G. Vlachos, M. P. Watson, M. C. Berg, T. H. Epps, L. S. T. J. Korley, *Annu. Rev. Mater. Res.* 2022, 52, 249–280.
- [7] C. Jehanno, J. W. Alty, M. Roosen, S. De Meester, A. P. Dove, E. Y. X. Chen, F. A. Leibfarth, H. Sardon, *Nature* 2022, 603, 803–814.
- [8] J. B. Williamson, S. E. Lewis, R. R. Johnson, I. M. Manning, F. A. Leibfarth, *Angew. Chem. Int. Ed.* 2019, 58, 8654–8668.
- [9] E. Blasco, M. B. Sims, A. S. Goldmann, B. S. Sumerlin, C. Barner-Kowollik, *Macromolecules* 2017, 50, 5215–5252.
- [10] N. K. Boaen, M. A. Hillmyer, Chem. Soc. Rev. 2005, 34, 267– 275.
- [11] N. M. G. Franssen, J. N. H. Reek, B. de Bruin, Chem. Soc. Rev. 2013, 42, 5809–5832.
- [12] G. W. Coates, Y. D. Y. L. Getzler, Nat. Rev. Mater. 2020, 5, 501–516.
- [13] P. R. Christensen, A. M. Scheuermann, K. E. Loeffler, B. A. Helms, *Nat. Chem.* 2019, 11, 442–448.
- [14] M. Hong, E. Y. X. Chen, Green Chem. 2017, 19, 3692-3706.
- [15] J. B. Zhu, E. M. Watson, J. Tang, E. Y. X. Chen, Science 2018, 360, 398–403.
- [16] S. E. Lewis, B. E. Wilhelmy, F. A. Leibfarth, Chem. Sci. 2019, 10, 6270–6277.
- [17] J. B. Williamson, W. L. Czaplyski, E. J. Alexanian, F. A. Leibfarth, Angew. Chem. Int. Ed. 2018, 57, 6261–6265.
- [18] J. B. Williamson, C. G. Na, R. R. Johnson, W. F. M. Daniel, E. J. Alexanian, F. A. Leibfarth, J. Am. Chem. Soc. 2019, 141, 12815–12823.
- [19] M. Zeng, Y. H. Lee, G. Strong, A. M. Lapointe, A. L. Kocen, Z. Qu, G. W. Coates, S. L. Scott, M. M. Abu-Omar, ACS Sustainable Chem. Eng. 2021, 9, 13926–13936.
- [20] D. E. Fagnani, D. Kim, S. I. Camarero, J. F. Alfaro, A. J. McNeil, Nat. Chem. 2023, 15, 222–229.
- [21] E. E. Stache, V. Kottisch, B. P. Fors, J. Am. Chem. Soc. 2020, 142, 4581–4585.
- [22] B. Slater, S. O. Wong, A. Duckworth, A. J. P. White, M. R. Hill, B. P. Ladewig, *Chem. Commun.* 2019, 55, 7319–7322.
- [23] P. T. Chazovachii, M. J. Somers, M. T. Robo, D. I. Collias, M. I. James, E. N. G. Marsh, P. M. Zimmerman, J. F. Alfaro, A. J. McNeil, *Nat. Commun.* 2021, 12, 4524.
- [24] C. P. Easterling, T. Kubo, Z. M. Orr, G. E. Fanucci, B. S. Sumerlin, *Chem. Sci.* 2017, 8, 7705–7709.
- [25] C. J. Hawker, K. L. Wooley, Science 2005, 309, 1200-1205.
- [26] A. D. Fried, B. J. Wilson, N. J. Galan, J. N. Brantley, J. Am. Chem. Soc. 2022, 144, 8885–8891.
- [27] S. E. Lewis, B. E. Wilhelmy, F. A. Leibfarth, *Polym. Chem.* 2020, 11, 4914–4919.
- [28] B. Adhikari, S. Maiti, Prog. Polym. Sci. 2000, 25, 909-948.



- [29] S. Ramarad, M. Khalid, C. T. Ratnam, A. L. Chuah, W. Rashmi, Prog. Mater. Sci. 2015, 72, 100–140.
- [30] Rubber Recycling: Challenges and Developments (Eds.: J. K. Kim, P. Saha, S. Thomas, J. T. Haponiuk, M. K. Aswathi), Royal Society of Chemistry, Cambridge, 2018.
- [31] Y. Ren, T. P. Lodge, M. A. Hillmyer, J. Am. Chem. Soc. 1998, 120, 6830–6831.
- [32] Y. Ren, T. P. Lodge, M. A. Hillmyer, Macromolecules 2001, 34, 4780–4787.
- [33] K. De Bruycker, M. Delahaye, P. Cools, J. Winne, F. E. D. Prez, Macromol. Rapid Commun. 2017, 38, 1700122.
- [34] D. Derouet, J. C. Brosse, L. Cauret, F. Morvan, S. Mulder-Houdayer, J. Appl. Polym. Sci. 2003, 87, 47–60.
- [35] V. A. Tanna, J. S. Enokida, E. B. Coughlin, H. H. Winter, *Macromolecules* 2019, 52, 6135–6141.
- [36] S. Wang, S. Zhang, C. Feng, G. Lu, P. Theato, X. Huang, C. Feng, *Polym. Chem.* 2021, 12, 5589–5597.
- [37] F. A. Soares, A. Steinbüchel, Macromol. Biosci. 2021, 21, 2100261.
- [38] S. Billiet, K. De Bruycker, F. Driessen, H. Goossens, V. Van Speybroeck, J. M. Winne, F. E. Du Prez, *Nat. Chem.* 2014, 6, 815, 821
- [39] S. Van Der Heijden, K. De Bruycker, R. Simal, F. Du Prez, K. De Clerck, *Macromolecules* 2015, 48, 6474–6481.
- [40] K. De Bruycker, S. Billiet, H. A. Houck, S. Chattopadhyay, J. M. Winne, F. E. Du Prez, Chem. Rev. 2016, 116, 3919–3974.
- [41] Y. Cao, K.D. Sayala, P. L. Gamage, R. Kumar, N. V. Tsarevsky. *Macromolecules* 2020, 53, 8020–8031.
- [42] R. E. Cohen, A. R. Ramos, Macromolecules 1979, 12, 131-134.
- [43] S. Daniele, A. Mariconda, G. Guerra, P. Longo, L. Giannini, Polymer 2017, 130, 143–149.

- [44] M. Mohadjer Beromi, C. R. Kennedy, J. M. Younker, A. E. Carpenter, S. J. Mattler, J. A. Throckmorton, P. J. Chirik, *Nat. Chem.* 2021, 13, 156–162.
- [45] W. P. Teh, D. C. Obenschain, B. M. Black, F. E. Michael, J. Am. Chem. Soc. 2020, 142, 16716–16722.
- [46] M. A. Hillmyer, S. B. T. Nguyen, R. H. Grubbs, *Macromole-cules* 1997, 30, 718–721.
- [47] T. Morita, B. R. Maughon, C. W. Bielawski, R. H. Grubbs, *Macromolecules* 2000, 33, 6621–6623.
- [48] J. A. Jaye, E. M. Sletten, Polym. Chem. 2021, 12, 6515-6526.
- [49] D. A. Adsmond, D. J. W. Grant, J. Pharm. Sci. 2001, 90, 2058– 2077.
- [50] W. Cooper, R. K. Smith, J. Polym. Sci. Part A 1963, 1, 159-168.
- [51] J. N. Short, G. Kraus, R. P. Zelinski, F. E. Naylor, *Rubber Chemistry and Technology*, American Chemical Society, Washington, 1959, pp. 614–627.
- [52] M. Berger, D. J. Buckley, J. Polym. Sci. Part A 1963, 1, 2945– 2964.
- [53] I. P. Parkin, R. G. Palgrave, J. Mater. Chem. 2005, 15, 1689– 1695.
- [54] P. Ragesh, V. Anand Ganesh, S. V. Nair, A. S. Nair, J. Mater. Chem. A 2014, 2, 14773–14797.
- [55] C. Wang, G. O. Brown, D. L. Burris, L. S. T. J. Korley, T. H. Epps, ACS Appl. Polym. Mater. 2019, 1, 2249–2266.
- [56] O. N. Tretinnikov, J. Adhes. Sci. Technol. 1999, 13, 1085–1102.

Manuscript received: March 1, 2023 Accepted manuscript online: March 16, 2023 Version of record online: April 12, 2023 3213773, 2023, 20, Downloaded from https://onlinelibary.wile.com/doi/10.1002/anie202303115 by University Of Washington, Wiley Online Library on [2207/2023]. See the Terms and Conditions (https://onlinelibrary.wiley.com/terms-and-conditions) on Wiley Online Library for rules of use; OA archies are governed by the applicable Creative Commons.